Journal of Power Sources 195 (2010) 662–666

Contents lists available at ScienceDirect

Journal of Power Sources

journal homepage: www.elsevier.com/locate/jpowsour

Short communication

# Electrochemical cell studies based on non-aqueous magnesium electrolyte for electric double layer capacitor applications

Ramasamy Chandrasekaran[a], Meiten Koh[b], Akiyoshi Yamauchi[b], Masashi Ishikawa[a,*]

[a] Department of Chemistry and Materials Engineering, Faculty of Chemistry, Materials and Bioengineering, Kansai University, 3-3-35 Yamate-cho, Suita 564-8680, Japan
[b] Chemical Division, Fundamental Research Department, Daikin Industries Ltd., 1-1 Nishihitotsuya, Settsu 565-8585, Japan

ARTICLE INFO

*Article history:*
Received 2 June 2009
Received in revised form 28 July 2009
Accepted 29 July 2009
Available online 5 August 2009

*Keywords:*
Electric double layer capacitor
Non-aqueous magnesium electrolyte
Lithium salt
Activated carbon
Specific capacitance

ABSTRACT

Performances of electric double layer capacitors (EDLCs) based on an activated carbon electrode with acetonitrile (ACN), propylene carbonate (PC), or a ternary electrolyte, i.e., PC:ethylene carbonate (EC):diethyl carbonate (DEC), at 1 mol $dm^{-3}$ of magnesium perchlorate [$Mg(ClO_4)_2$] salt have been investigated. The electrochemical responses were studied by impedance spectroscopy, cyclic voltammetry, and galvanostatic charge–discharge experiments at 25 °C in a three-electrode configuration. For a comparative evaluation, lithium perchlorate ($LiClO_4$) salt-based systems were also evaluated. All the observed results showed typical EDLC characteristics within the potential range between 0 and 1 V vs. an $Ag/Ag^+$ reference electrode. The Mg-based systems exhibited similar or rather better performances than the corresponding Li-based electrolytes; in particular, the rate capability of Mg-based ACN and PC electrolytes was much better than the corresponding Li-based electrolytes, indicating the high accessibility and utility of activated carbon pores by solvated Mg ions.



## 1. Introduction

During the last three decades, considerable interest has been focused on the development of electrochemical capacitors for energy storage devices and hybrid electric vehicles. Electric double layer capacitors (EDLCs) have been widely adopted due to their conventional applicability [1]. A major constituent of EDLC electrode materials is carbonaceous materials. The materials are widely applied in different and still attractive forms. Among them, activated carbon is one of the most promising electrode materials because of its low cost, high surface area, structural stability and electrochemical inertness within a wide potential window [2]. Their capacitance change emerges with a difference not only in the surface area but also in their pore size distribution (PSD), i.e., meso- and micro-pore proportions [3–5].

In order to achieve a high energy density EDLC, an organic electrolyte system is considered instead of aqueous electrolytes. Various organic solvents have been applied to non-aqueous systems, which offer sufficient electrochemical stability and commercial applications. In particular, cyclic and aliphatic carbonates such as propylene carbonate (PC), ethylene carbonate (EC) and diethyl carbonate (DEC) have been extensively studied in secondary battery and capacitor applications [6]. Acetonitrile (ACN) has higher conductivity than other conventional organic solvents, but its use is ill-advised due to its toxic nature [7].

Li-based electrochemical systems have played a vital role for the past three decades due to their high specific energy densities. Unfortunately, they have certain drawbacks such as requiring unconventional handling and being high cost economically. Accordingly, magnesium (Mg) electrochemistry has attracted interest in electrochemical research and development due to its electrochemical properties, abundance of resources, low cost and low environmental hazardousness [8]. Mg-based systems have a specific capacity between lithium (Li) and nickel–cadmium (Ni–Cd) systems [9]. Nonetheless, their usage has been limited due to slower Mg-ion diffusion and non-conductive film formation during the cell cycling, which reduces cell capacity cycle by cycle [10]. Therefore, we have to optimize the working nature of Mg-based systems by modification of electroactive components [11] and also consider merits like Mg-ion stability, its small ionic size and lower reactivity than elements of the alkali metal series [12].

Very few reports on Mg-based electrolytes in electrochemical capacitors can be found in the literature; these reports evidenced the role of Mg salts in polymer and aqueous electrolytes [1,13,14]. Though satisfied the conduction level of Mg-based polymer electrolytes was accomplished due to its high carrier concentration compensating for its slow mobility, which lifts the conductivity to the level of Li-based systems [15], there is no relevant report available on an Mg electrolyte system for activated carbon-based organic EDLC cells. In this article, we focus

* Corresponding author. Tel.: +81 6 6368 0952; fax: +81 6 6368 0952.
*E-mail address:* masaishi@ipcku.kansai-u.ac.jp (M. Ishikawa).

0378-7753/$ – see front matter © 2009 Elsevier B.V. All rights reserved.
doi:10.1016/j.jpowsour.2009.07.043

on the design and characteristics of an electrochemical capacitor by using an Mg-based electrolyte to explore its utility for EDLC applications.

## 2. Experimental

The starting materials, activated carbon (NK260, Kuraray Chemical Co., Ltd., specific surface area: 2040 $m^2\,g^{-1}$, average pore diameter: 1.92 nm) and carbon black (Denka Black, Denki Kagaku Kogyo Co., Ltd.) were dried at 120 °C for 12 h before use. The electrodes were prepared by mechanically mixing activated carbon with carbon black and polyvinylidene fluoride (PVdF) as binder in *N*-methylpyrrolidinone (NMP) at a weight ratio of 8:1:1. The obtained slurry was coated on a platinum sheet with a thickness of around 200 μm in a 1 $cm^2$ area and dried at 120 °C for 12 h under a vacuum condition. The thickness of the heated electrodes was kept approximately between 50 and 60 μm and the weight of the activated carbon was adjusted between 2 and 3 mg, which excluded carbon black and binder weight. A typical symmetric form capacitor was assembled in a home-made square-type Teflon three-electrode cell with the two carbon electrodes, which were separated by a glass fiber separator (GB100R, Toyo Roshi Kaisha Ltd.). An $Ag/Ag^+$ electrode in an $AgNO_3$-saturated ACN solution was used as a reference electrode. The Mg perchlorate [$Mg(ClO_4)_2$] (Wako Chemical Co., Ltd.) based electrolytes containing different organic solvents were applied. The prepared electrolyte systems were as follows: (i) 1 mol $dm^{-3}$-$Mg(ClO_4)_2$-ACN, (ii) 1 mol $dm^{-3}$-$Mg(ClO_4)_2$-PC, (iii) 1 mol $dm^{-3}$-$Mg(ClO_4)_2$-EC:DEC:PC (1:1:1, v/v/v), (iv) 1 mol $dm^{-3}$-$LiClO_4$-ACN, (v) 1 mol $dm^{-3}$-$LiClO_4$-PC, and (vi) 1 mol $dm^{-3}$-$LiClO_4$-EC:DEC:PC (1:1:1, v/v/v); hereafter mol $dm^{-3}$ is abbreviated to M.

All the electrochemical experiments were carried out using a Solartron 1480 multistat-electrochemical analyzer with Corrware II software (Scribner Associates) at temperature 25 °C. Electrochemical impedance spectroscopy (EIS) was performed in a frequency range from 20,000 to 0.01 Hz at a sinusoidal source with an amplitude of 10 mV. The specific capacitance $C$ (F $g^{-1}$) from the EIS plots was calculated from the formula: $C = -2/(2\pi f Z'' m)$, where $Z''$ is the imaginary part of the total complex impedance (Ω), $m$ is the working (positive) electrode weight, and $f$ is the frequency (Hz). Cyclic voltammetry (CV) experiments were carried out in a potential window between 0 and 1 V at scan rates of 10 and 50 mV $s^{-1}$. The specific capacitance $C$ (F $g^{-1}$) was calculated by using the equation: $C = i/(mv)$, where $i$ is an average value of anodic–cathodic currents, $m$ is the working (positive) electrode weight, and $v$ is the corresponding scan rate. Galvanostatic charge–discharge of the electrode was performed at different current densities specifically at 500, 1000, 2000 and 3000 mA $g^{-1}$. The specific capacitance $C$ (F $g^{-1}$) was calculated from the obtained charge–discharge curves by using the formula: $C = I\Delta t/\Delta V m$, where $I$ is the applied current, $\Delta t$ is the time period, and $\Delta V$ is the operation potential width.

## 3. Results and discussion

Fig. 1(a) shows Nyquist plots for the capacitors based on the Mg electrolytes, and Fig. 1(b) shows them for the behavior with the corresponding Li electrolyte-based systems. It is clearly shown that typical carbon-based EDLC impedance plots are observed in all systems, i.e., a high-frequency semicircle with a low-frequency line to the tail end. This implies that the Mg electrolytes are applicable to EDLC just like the Li electrolytes. Curves 1, 2 and 3 in Fig. 1(a) represent the plots for the cells based on 1 M $Mg(ClO_4)_2$ in ACN, PC and EC:DEC:PC (1:1:1) electrolytes, respectively. An internal resistance (*R*s, intercept point to the real axis), which is derived from

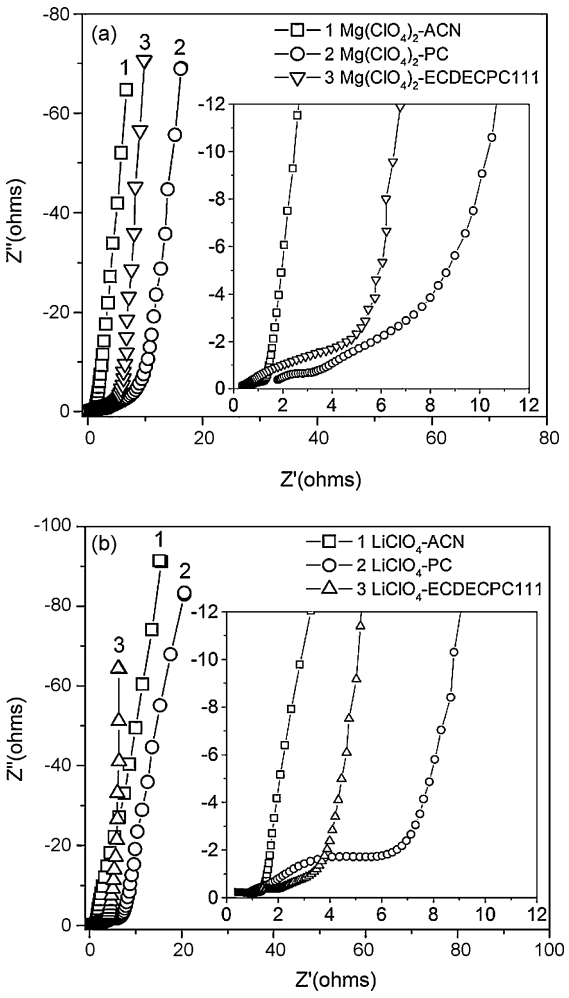


**Fig. 1.** Complex impedance–Nyquist plots for the activated carbon cells with (a) Mg-based electrolytes and (b) Li-based electrolytes.

the electroactive components and the electrical circuit of EDLC [16], is found to be 0.36, 1.75 and 0.41 Ω for the cells based on the electrolytes 1 M $Mg(ClO_4)_2$ in ACN, PC and EC:DEC:PC (1:1:1), respectively, whereas the observed *R*s values for the respective $LiClO_4$ electrolyte-based cells are 0.45, 0.89 and 0.92 Ω. They all show favorably low resistivity.

A polarization resistance $R_P$ was determined from the apparent diameter of a semicircle from an impedance curve. The measured $R_P$ values are 0.56, 1.33 and 1.38 Ω for the Mg-based cells while 0.52, 5.10 and 0.88 Ω for the Li-based systems. Usually, a lower value of $R_P$ is more pronounced ideal double layer capacitive behavior. A considerable solvent effect on the resistance is observed when ACN-based systems are compared with PC-based cells, which is absolutely due to the viscosity of the corresponding electrolytes (see viscosities in Table 1). They are reflected in the penetration process of ions into an electrode from the mid to low frequency regions [7,17].

In the low frequency region, observed are not only lower resistance (along the real axis) but also a smaller imaginary value of the Mg-based systems than the Li-based systems; the latter means higher capacitance by the Mg-based electrolytes when compared to the Li-based electrolytes. From these impedance data, specific capacitance values are found to be 219.6, 180.2 and 176.0 F $g^{-1}$ for the cells based on 1 M $Mg(ClO_4)_2$-ACN, -PC and -EC:DEC:PC (1:1:1), while the values are 198.0, 154.1 and 237.8 F $g^{-1}$ for the cells based on 1 M $LiClO_4$-ACN, -PC and -EC:DEC:PC (1:1:1), respectively. These

**Table 1**
Selected specific capacitance for Mg and Li electrolyte-based EDLCs and their electrolyte viscosity.

| Electrolyte system | Charge–discharge rate ($mA\,g^{-1}$) | | | | |
|---|---|---|---|---|---|
| | 500 | 1000 | 2000 | 3000 | Viscosity (mPa s) at 25 °C |
| | Capacitance ($F\,g^{-1}$) | | | | |
| Mg electrolyte | | | | | |
| 1 M-$Mg(ClO_4)_2$-ACN | 161.6 | 154.6 | 147.2 | 142.2 | 1.62 |
| 1 M-$Mg(ClO_4)_2$-PC | 147.9 | 137.4 | 118.0 | 111.6 | 29.20 |
| 1 M-$Mg(ClO_4)_2$-EC:DEC:PC | 169.5 | 162.0 | 148.0 | 144.1 | 18.80 |
| Li electrolyte | | | | | |
| 1 M-$LiClO_4$-ACN | 143.6 | 134.0 | 115.2 | 106.8 | 0.88 |
| 1 M-$LiClO_4$-PC | 126.5 | 113.4 | 100.8 | 95.4 | 8.02 |
| 1 M-$LiClO_4$-EC:DEC:PC | 176.1 | 175.0 | 171.0 | 174.0 | 5.05 |

values suggest that capacitances generated in the Mg systems are comparable to those obtained in the Li systems; surprisingly, some values based on Mg are rather higher than those observed in the Li systems. These calculated capacitances under a small polarization condition (10 $mV_{p-p}$) are sometimes not strictly correlative to the values by macroscopic polarization, such as CV and galvanostatic cycling. Therefore, we should also confirm capacitances in such conditions.

Fig. 2(a)–(d) shows the typical recorded CVs of the capacitors: Fig. 2(a) and (c) represents the capacitors containing the Mg electrolytes at scan rates of 10 and 50 $mV\,s^{-1}$, respectively, whereas (b) and (d) displays the capacitors based on the corresponding Li electrolyte systems. At the lower scan rate of 10 $mV\,s^{-1}$ [Fig. 2(a) and (b)], although fairly ideal capacitive behavior is observed in both the Mg and Li systems, there is an *I–V* variant at the terminal potentials (0 and 1.0 V), except for the $Mg(ClO_4)_2$-ACN and $LiClO_4$-EC:DEC:PC systems. That would be ascribed to diffusion limitation in meso- and micro-pores at scan direction switching. Ion penetration at the pores must be more difficult at a higher scan rate of 50 $mV\,s^{-1}$, and hence noticeable current distortion as shown in Fig. 2(c) and (d) [18,19]. Note that the observed good exceptions, $Mg(ClO_4)_2$-ACN and $LiClO_4$-EC:DEC:PC systems, correlate with the overall lowest impedance systems in Fig. 1.

The PC-based systems show lower current density than the others with regard to the respective cations. This effect would reflect low accessibility of PC-solvated ions at carbon electrodes as observed also in the impedance measurement (Fig. 1). No evidence of redox currents and uniform *I–V* responses in the sweep region are observed during repeated runs, indicating dominant electric double layer capacitance. The calculated specific capacitance values are 170.9 and 150.4 for ACN-, 148.4 and 114.8 for PC-, 177.7 and 136.5 $F\,g^{-1}$ for EC:DEC:PC-Mg salt systems at the scan rates of 10 and 50 $mV\,s^{-1}$, respectively. These values for the Mg systems are mostly higher than the corresponding Li-based system values; the calculated specific capacitances of the Li-based cells are 145.0 and 113.8 for ACN-, 124.7 and 96.8 for PC-, 169.0 and 148.0 $F\,g^{-1}$ for PC:EC:DEC-based cells at the respective scan rates of 10 and 50 $mV\,s^{-1}$. It is notable that the ternary solvent systems exhibit comparable or rather higher capacitances than ACN-based systems, especially at the lower scan rate. Overall, the highest capacitance is obtained for the EC:DEC:PC-based Mg electrolyte (177.7 $F\,g^{-1}$) at 10 $mV\,s^{-1}$.

The electrochemical storage behaviors of EDLCs were also examined under constant-current charge–discharge conditions. Fig. 3(a)–(f) shows voltage–time (*V–t*) response of the Mg

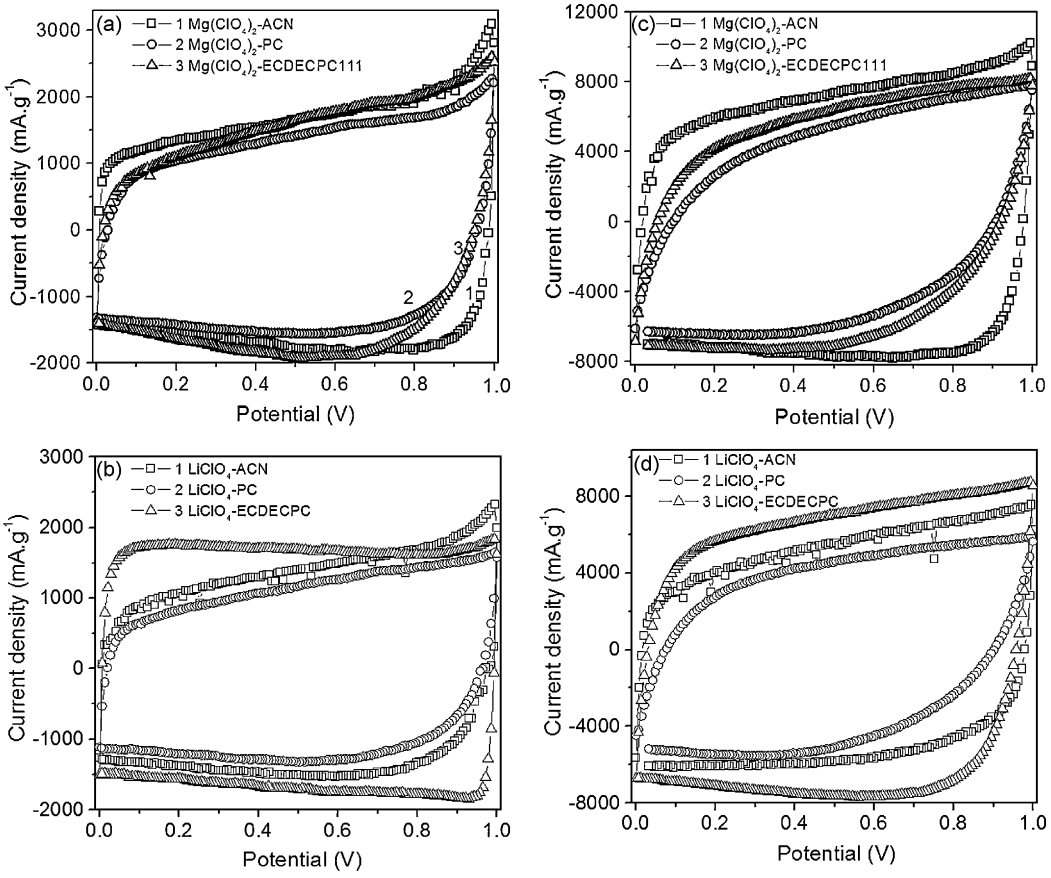


**Fig. 2.** Typical cyclic voltammograms for the cells based on 1 M $Mg(ClO_4)_2$ in AN, PC and EC:DEC:PC (1:1:1) at (a) 10 $mV\,s^{-1}$ and (c) 50 $mV\,s^{-1}$; based on 1 M $LiClO_4$ in AN, PC and EC:DEC:PC (1:1:1) at (b) 10 $mV\,s^{-1}$ and (d) 50 $mV\,s^{-1}$.

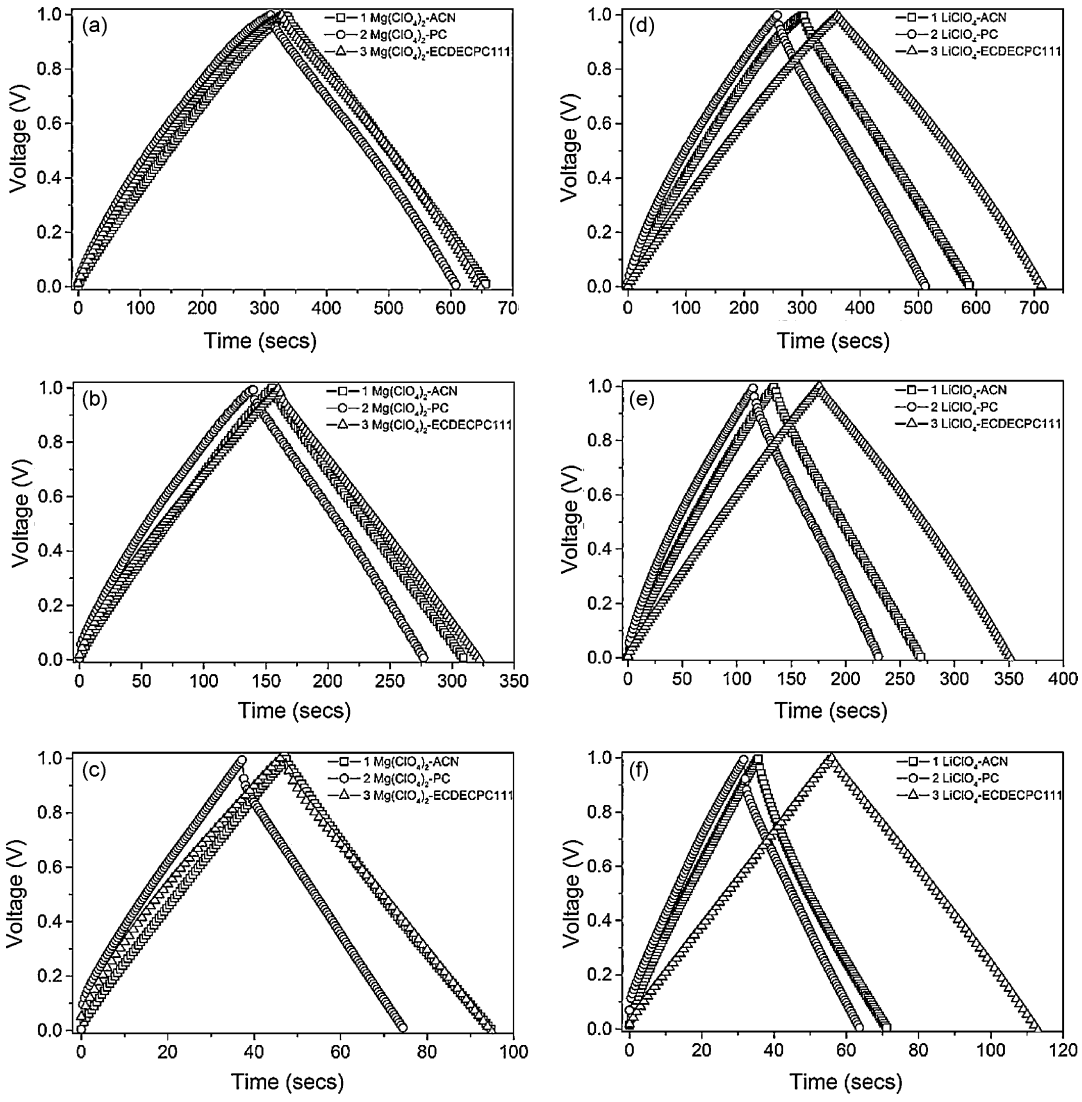


**Fig. 3.** Galvanostatic charge–discharge curves for capacitors with Mg-based electrolytes at (a) 500 mA $g^{-1}$, (b) 1000 mA $g^{-1}$ and (c) 3000 mA $g^{-1}$; with Li-based electrolytes at (d) 500 mA $g^{-1}$, (e) 1000 mA $g^{-1}$ and (f) 3000 mA $g^{-1}$.

[Fig. 3(a)–(c)] and Li [Fig. 3 (d)–(f)] electrolyte-based capacitors at current densities: 500, 1000 and 3000 mA $g^{-1}$. Almost linear *V–t* dependence demonstrates the typical double layer capacitive behavior of the cells. The curves in Fig. 3(a) represent the behaviors of the cells with 1 M $Mg(ClO_4)_2$-ACN, -PC and -EC:DEC:PC at the lowest charge–discharge rate of 500 mA $g^{-1}$, where their respective specific capacitances are 161.6, 147.9 and 169.5 F $g^{-1}$. The corresponding Li-based electrolyte systems exhibit similar or rather lower capacitance than the Mg-based systems as shown in Fig. 3(d).

Fig. 3(b) and (c) represents the charge–discharge curves for the Mg-based cells at higher rates of 1000 and 3000 mA $g^{-1}$, respectively, while (e) and (f) shows the corresponding results for Li electrolyte-based cells. The estimated specific capacitance values are listed in Table 1, which also indicates the results at 2000 mA $g^{-1}$. From Fig. 3 and Table 1, one can see the high-rate compatibility of the Mg-based electrolytes when compared to the Li electrolyte-based cell. Among the Li electrolytes, only the ternary carbonate solvent system shows an excellent rate capability. The discharge capacitances of the present activated carbon with 1.96 M triethylmethylammonium tetrafluoroborate ($TEMABF_4$) dissolved in PC as a common EDLC electrolyte are 151.6 and 143.4 F $g^{-1}$ at 500 and 1000 mA $g^{-1}$, respectively [20]. Thus the present Mg electrolyte systems can be considered comparable to a common ammonium electrolyte.

Better performance of the Mg-based electrolytes in the CVs as well as galvanostatic studies suggests that Mg ion does not suffer the intense solvation that causes an increase in Stokes' radius and hence a decrease in mobility as well as in pore utility when compared to Li ion. Usually at higher rates, a sharp voltage change, namely *IR* drop, would be observed at the beginning and termination of a charge–discharge process due to the equivalent series resistance (ESR) of a capacitor, and thus the lower capacitance would be obtained due to a decrease in pore accessibility of ions [21]. However, observed *IR* drop is very small for the Mg systems even at the highest charge–discharge rate of 3000 mA $g^{-1}$, indicating that ESR of the capacitors is low enough. Obvious *IR* drop is only found in the PC electrolyte-based cells with Mg ion as well as Li ion. Interestingly, the Mg-PC system still exhibits much better capacitance than the Li-PC system, probably meaning that the smaller Stokes' radius of Mg ion enhances pore utility more than that of Li ion, at least in the pores. The future direction of this study will focus on this detailed mechanism. The capacitance retention of three Mg-based electrolyte systems was also examined in long-term 500 cycling at 1000 mA $g^{-1}$; no severe loss of capacitance was

observed in the Mg-based cells (3–6%) like Li-based systems (1–5%), i.e., no obvious demerits of $Mg^{2+}$ were evidenced.

## 4. Conclusion

The outcomes of charge–discharge studies and voltammograms of the Mg electrolytes have shown the absence of redox processes and of nonlinearity functions. These results indicate that a good electrode/electrolyte interface is accomplished for the double layer mechanisms. Electrolyte performance in EDLC with porous carbon materials depends on the pore distribution and structure. In this work, although we have not optimized the pore structure for Mg ion in the electrolytes and its interaction with the electrode, we can find a similar or better accessibility of divalent Mg ion like monovalent Li ion, which leads to a focus on research utilizing such a non-aqueous Mg electrolyte and some intercalation Mg materials together with an activated carbon electrode.

## Acknowledgements

This work was supported by Grant-in-Aid for Scientific Research B and the "Strategic Project to Support the Formation of Research Bases at Private Universities": Matching Fund Subsidy from MEXT (the Ministry of Education, Culture Sports, Science and Technology of Japan). We would thank Mr. Atsushi Yamaguchi for his viscosity measurement.

## References

[1] R. Chandrasekaran, M. Koh, A. Yamauchi, M. Ishikawa, Electrochemistry 77 (2009) 51.
[2] R. Chandrasekaran, Y. Soneda, J. Yamashita, M. Kodama, H. Hatori, J. Solid State Electrochem. 12 (2008) 1349.
[3] K. Yang, S. Yiacoumi, C. Tsouris, J. Electroanal. Chem. 540 (2003) 159.
[4] F. Wu, R. Tseng, C. Hu, C. Wang, J. Power Sources 159 (2006) 1532.
[5] V. Ruiz, C. Blanco, R. Santamaria, J.M. Juráz-Galán, A. Sepulveda-Escribano, F. Rodriguez-Reinso, Micropor. Mesopor. Mater. 110 (2008) 431.
[6] R. Chandrasekaran, Y. Ohzawa, T. Nakajima, M. Koh, H. Aoyama, J. New Mater. Electrochem. Syst. 9 (2006) 181.
[7] A. Jänes, E. Lust, J. Electroanal. Chem. 588 (2006) 285.
[8] O. Chusid, Y. Gofer, H. Gizbar, Y. Vestfrid, E. Levi, D. Aurbach, I. Riech, Adv. Mater. 15 (2003) 627.
[9] Y. NuLi, Z. Guo, H. Liu, J. Yang, Electrochem. Commun. 9 (2007) 913.
[10] N. Amir, Y. Vestfrid, O. Chusid, Y. Gofer, D. Aurbach, J. Power Sources 174 (2007) 1234.
[11] P. Novák, R. Imhof, O. Haas, Electrochim. Acta 45 (1999) 351.
[12] N. Imanaka, Y. Okazaki, G. Adachi, J. Mater. Chem. 10 (2000) 1431.
[13] S. Mitra, A.K. Shukla, S. Sampath, J. Power Sources 101 (2001) 213.
[14] D. Imamura, M. Miyayama, Solid State Ionics 161 (2003) 173.
[15] M. Morita, F. Araki, K. Kashiwamura, N. Yoshimoto, M. Ishikawa, Electrochim. Acta 45 (2000) 1335.
[16] P.L. Taberna, P. Simon, J.F. Fauvarque, J. Electrochem. Soc. 150 (2003) A292.
[17] M. Arulepp, L. Permann, J. Leis, A. Perkson, K. Rumma, A. Jänes, E. Lust, J. Power Sources 133 (2004) 320.
[18] A.G. Pandolfo, A.F. Hollenkamp, J. Power Sources 157 (2006) 11.
[19] C. Vix-Guterl, E. Frackowiak, K. Jurewicz, M. Friebe, J. Parmentier, F. Beĭguin, Carbon 43 (2005) 1293.
[20] M. Suenaga, M. Ishikawa, unpublished data.
[21] G. Gryglewicz, J. Machnikowski, E. Lorenc-Grabowska, G. Lota, E. Frackowiak, Electrochim. Acta 50 (2005) 1197.